Journal of
Synchrotron
Radiation

ISSN 0909-0495

Received 30 November 2011
Accepted 18 June 2012

Grazing-incidence X-ray diffraction study of rubrene epitaxial thin films

Enrico Fumagalli,[a]* Marcello Campione,[b] Luisa Raimondo,[a] Adele Sassella,[a] Massimo Moret,[a] Luisa Barba[c] and Gianmichele Arrighetti[c]

[a]Department of Materials Science, University of Milano-Bicocca, via R. Cozzi 53, I-20125 Milano, Italy, [b]Department of Geological Sciences and Geotechnologies, University of Milano-Bicocca, Piazza della Scienza 4, I-20126 Milano, Italy, and [c]Institute of Crystallography, ELETTRA, CNR, SS 14 Km 163.5, Area Science Park, 34012 Basovizza, Trieste, Italy.
E-mail: enrico.fumagalli@mater.unimib.it

The growth of organic semiconductors as thin films with good and controlled electrical performances is nowadays one of the main tasks in the field of organic semiconductor-based electronic devices. In particular it is often required to grow highly crystalline and precisely oriented thin films. Here, thanks to grazing-incidence X-ray diffraction measurements carried out at the ELETTRA synchrotron facility, it is shown that rubrene thin films deposited by organic molecular beam epitaxy on the surface of tetracene single crystals have the structure of the known orthorhombic polymorph, with the (2 0 0) plane parallel to the substrate surface. Moreover, the exact epitaxial relationship between the film and the substrate crystalline structures is determined, demonstrating the presence of a unique in-plane orientation of the overlayer.

Keywords: GIXD; thin films; epitaxy.

1. Introduction

Nowadays organic semiconducting materials attract great attention due to their possible exploitation in the fabrication of electronic devices in substitution to the now widely employed inorganic semiconductors, owing to the cheaper and easier processing they require and to the possibility of easily tuning their physical properties (Braga & Horowitz, 2009; Brütting, 2006; Wöll, 2009; Rand *et al.*, 2007). One of the main shortcomings in the use of this class of materials in electronic devices are their poor electrical transport properties, if compared with their inorganic counterparts. For this reason the studies have been focused on materials which exhibit particularly high charge-carrier mobility (Klauk *et al.*, 2002; Yamashita, 2009) and on the improvements of their structural properties, with advantages over all solid state properties. Among those materials rubrene (RUB, $C_{42}H_{28}$, 5,6,11,12-tetraphenyltetracene) has emerged as one of the most promising organic semiconductors, having a charge-carrier mobility of 30 $cm^2\ V^{-1}\ s^{-1}$, close to that of amorphous silicon (Podzorov *et al.*, 2004). Such high mobility values, however, can be reached only when RUB molecules are in the highly ordered orthorhombic crystalline phase. Owing to this crystal structure, the transport properties of RUB crystals are also strongly anisotropic. In order to exploit RUB in the fabrication of micro-electronic devices it is thus necessary to be able to grow RUB highly crystalline thin films, with controlled crystalline orientation. Up to this moment the growth of high-quality RUB crystalline thin films has revealed to be a difficult task to accomplish (Käfer & Witte, 2005). Several authors have reported the successful growth of RUB crystalline thin films on Au substrates, on Bi substrates, on various inorganic substrates previously covered by a pentacene buffer layer and on some organic single crystals (Haemori *et al.*, 2005; Campione, 2008; Campione *et al.*, 2009; Lan *et al.*, 2011; Hu *et al.*, 2008). In the latter case, besides demonstrating the growth of crystalline RUB thin films, the epitaxial relationship was determined. However, the overlayer often presents a multitude of rotational domains.

Here, thanks to grazing-incidence X-ray diffraction (GIXD) measurements, a technique which already proved to be useful in the study of organic thin films (Smilgies *et al.*, 2005; Yoshida & Sato, 2006; Hu *et al.*, 2008), we study the structure of RUB crystalline thin films grown on tetracene (TEN) single crystals by organic molecular beam epitaxy (Sassella *et al.*, 2008). We show that such films have a high degree of crystallinity and grow with a unique crystalline orientation both in the in-plane and out-of-plane directions. In addition we also show that the experimental set-up of the beamline XRD1 at ELETTRA is suitable for carrying out GIXD characterization of the crystalline structure and orientation of organic crystalline thin films with a thickness down to less than 20 nm.

2. Experimental

2.1. Sample preparation

The samples used in this work consist of RUB (a = 26.86 Å, b = 7.193 Å, c = 14.433 Å, *Cmca*; Jurchescu *et al.*, 2006) epitaxial thin films grown on the (0 0 1) surface of triclinic TEN single crystals (a = 6.06 Å, b = 7.84 Å, c = 13.01 Å, α = 77.13°, β = 72.12°, γ = 85.79°, $P\bar{1}$; Holmes *et al.*, 1999). TEN single crystals are grown from commercial powder (Sigma–Aldrich, 99.9%) by physical vapour transport (Laudise *et al.*, 1998), with a constant nitrogen flux of 20 ml min^{-1} and with a source temperature of 459 K. In this way TEN single crystals with lateral dimensions up to a few millimetres and with a thickness of few hundreds of nanometres are obtained. The crystals are then placed on the surface of (1 0 0) silicon wafers, to which they spontaneously adhere. The epitaxial growth of the RUB thin films over the TEN substrates is then achieved by organic molecular beam epitaxy, a technique which gives great control over all the growth parameters. The deposition process is carried out in high vacuum (bare pressures at about 10^{-7} mbar), with a source temperature of 453 K, leading to a constant deposition rate of about 2 Å min^{-1}, as monitored by a quartz microbalance. The substrate is kept at room temperature. All the samples have a nominal thickness of 20 nm, and their surface morphology was checked immediately after the deposition with atomic force microscopy, showing a uniform coverage of the substrate surface by a highly crystalline RUB film, as shown elsewhere (Campione, 2008; Campione *et al.*, 2009).

2.2. GIXD experimental set-up

In a GIXD experiment a monochromatic X-ray beam is directed toward the sample surface with a very low (grazing) angle of incidence, in order to maximize the diffraction from the overlayer, at the same time minimizing the diffraction from the substrate. The GIXD measurements described in this work have been carried out at the XRD1 beamline of the ELETTRA synchrotron facility (Trieste, Italy). In our geometry (see Fig. 1) the X-ray beam direction is fixed, while the sample holder can be rotated about the different diffractometer axes, in order to reach the sample surface alignment in the horizontal plane containing the X-ray beam, and subsequently rotate it around an axis perpendicular to this plane or, alternatively, vary the angle between beam and surface (angle of incidence α_i). The diffracted pattern is then collected by a two-dimensional CCD detector (165 mm MarResearch) perpendicular to the incident beam, which allows the simultaneous collection of the whole diffraction pattern. For the measurements described in this work the X-ray beam has a wavelength of 0.99987 Å, selected from the white emission spectrum of the wiggler source by a double-crystal Si(111) monochromator, and the number of photons per second in the incident beam is 2.8×10^{10}. The beam cross section at the sample is limited by double slits to 0.2 mm both in the horizontal and vertical directions and forms an angle $\alpha_i = 0.2°$ with the surface of the sample. The collected images are integrated and corrected for Lorentz/polarization and for detector geometry, misalignments and distortions using the software *Fit2D* (Hammersley, 1997) by means of calibration diffraction patterns obtained from standard samples. The simulation of the two-dimensional GIXD patterns has been carried out by using the Mathematica package *NANOCELL* (Tate *et al.*, 2006) while the pole figures have been simulated with the software *STEREOPOLE* (Salzmann & Resel, 2004).

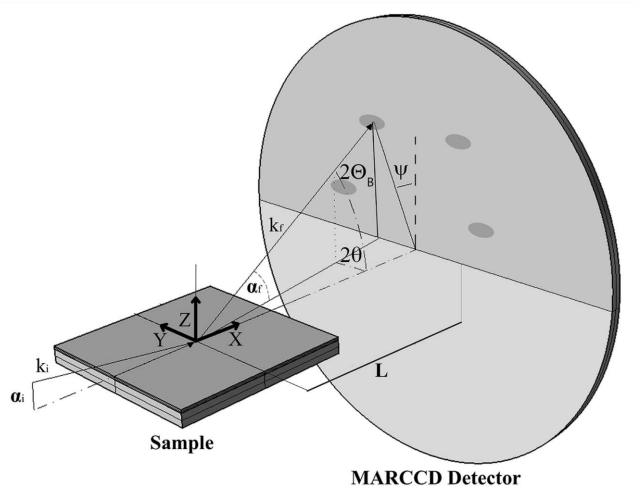

Figure 1
Geometry of the GIXD set-up. The incident beam forms an angle α_i with the sample surface and the diffracted beam is recorded by a planar CCD detector at a distance L from the beam incidence point. α_f and 2θ indicate the out-of-plane and in-plane diffraction angles, respectively, $2\Theta_B$ is the Bragg angle, ψ is the polar angle and X, Y and Z are the coordinates of the laboratory reference frame.

3. Results and discussion

3.1. Out-of-plane film orientation

In order to identify the different phases of a crystalline molecular thin film the first step is to carry out 'survey scans', in which the sample is rotated around the surface normal (Z) while the pattern is being collected (Smilgies & Blasini, 2007). In Fig. 2 a GIXD diffraction pattern collected while rotating the sample by a full turn about the normal to the sample surface, for a total exposure time of 1400 s, is shown. In general, such patterns are a superposition of the diffraction patterns originated by the different crystalline planes of the overlayer and substrate structures. In order to identify the origin of the various spots constituting the observed pattern we compared it with simulated GIXD patterns originating from the different materials constituting the sample. In Fig. 2 the simulated diffraction pattern of polycrystalline orthorhombic RUB with the (2 0 0) plane parallel to the substrate surface [as can be supposed considering the data reported by Campione (2008)] and with random azimuthal orientation of the grains (in order to account for the sample rotation during the measurement) is superimposed in black on the experimental pattern, while the simulated pattern of polycrystalline TEN with the same out-of-plane orientation as our substrate is shown in green. For both patterns some of the pertinent crystallographic indexes are also reported [in accordance with

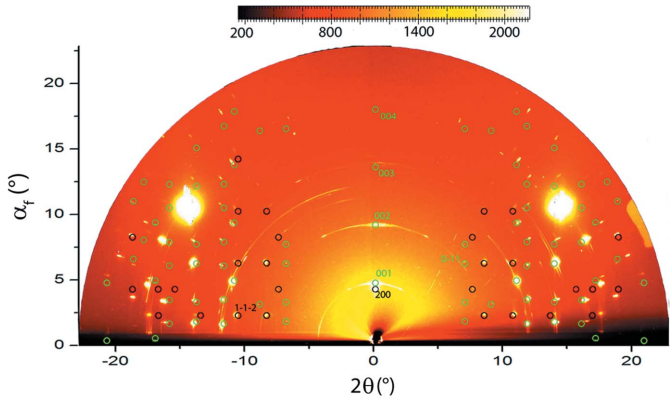

Figure 2
Two-dimensional GIXD pattern collected while rotating the sample by a full turn about the normal to the sample surface. The circles superimposed on the CCD image represent the position of the simulated diffraction spots from polycrystalline TEN with the (001) planes parallel to the sample surface (green circles), and from polycrystalline RUB with the (200) planes parallel to the sample surface (black circles). Also, the Miller indices of the reflections cited in the text are reported. The positions of the peaks in the experimental image are not corrected for detector misalignments.

the structures reported by Jurchescu *et al.* (2006) and Holmes *et al.* (1999)]. The presence of many spots originating from the substrate is due to the extremely low thickness of the RUB film, while the two larger spots originate from the silicon crystal used as substrate. It can be noticed that the whole measured pattern can be obtained by the superposition of the two simulated diffraction patterns, with no spots being left out. This means that the substrate is indeed crystalline TEN and, moreover, that the RUB thin film is entirely formed by molecules packed in the RUB orthorhombic crystalline phase, all with the same out-of-plane orientation, *i.e.* with the RUB (2 0 0) plane parallel to the surface of the substrate. Hence, we can rule out the presence of other RUB polymorphs in the film. The progressive deviation of the positions of the observed spots with respect to the simulated ones with the increase of the distance from the centre is due to a non-perfect orthogonality of the detector with respect to the incident beam. This effect can be corrected thanks to the calibration procedure, which indeed leads to a good correspondence also for the higher-order reflections (see Table 1, where the corrected positions of the out-of-plane peaks are reported). In Fig. 3 the central vertical region of a GIXD pattern, corresponding to the out-of-plane reflections, is reported. Below the two-dimensional CCD image, the one-dimensional diffraction pattern obtained by radial integration and calibration of the two-dimensional pattern is shown. The positions of the four peaks visible in the pattern are reported in Table 1, along with the calculated positions of the corresponding RUB (h 0 0) and TEN (0 0 l) reflections. The first peak corresponds to the (2 0 0) reflection of the orthorhombic phase of RUB, which is the only reflection originating from the (h 0 0) family of planes of the orthorhombic RUB crystal with a non-negligible intensity. The three other peaks correspond to the reflections originating from the (0 0 1), (0 0 2) and (0 0 3) planes of the TEN crystalline phase. The measured peak

Table 1
Experimental positions of the peaks (converted to the corresponding lattice spacing d) observed in the diffractogram in Fig. 3.

In the third column the Miller indices corresponding to each peak are reported, and in the fourth column the calculated position for each reflection is reported. In the fifth column the relative difference between calculated and measured peak positions is reported.

Peak number	Measured position (Å)	Corresponding reflection	Calculated position (Å)	Δ (%)
1	13.47112	RUB (200)	13.43000	0.3
2	12.25517	TEN (001)	12.10344	1.3
3	6.13478	TEN (002)	6.05172	1.4
4	4.08760	TEN (003)	4.03448	1.3

positions are in good agreement with the calculated ones and the larger shift between measured and calculated positions of the TEN diffraction peaks, with respect to the RUB peak, can be accounted for by noticing that the calculated peak positions for TEN are derived from the data reported by Holmes *et al.* (1999), which refers to measurements carried out at 175 K, while our measurements are carried out at room temperature. These data thus confirm that the TEN crystals used as substrate expose the (0 0 1) surface, and that RUB thin films are grown with the (2 0 0) crystallographic plane parallel to the substrate surface.

Finally, one can also observe the presence of some ring-like features, mainly originating from the out-of-plane TEN diffraction spots and from some other bright spot. On the other hand, there is no ring associated with the RUB diffraction spots. Such ring-like features indicate the presence of a high degree of texture of some parts of the sample and are probably due to disordered fragments of TEN crystals

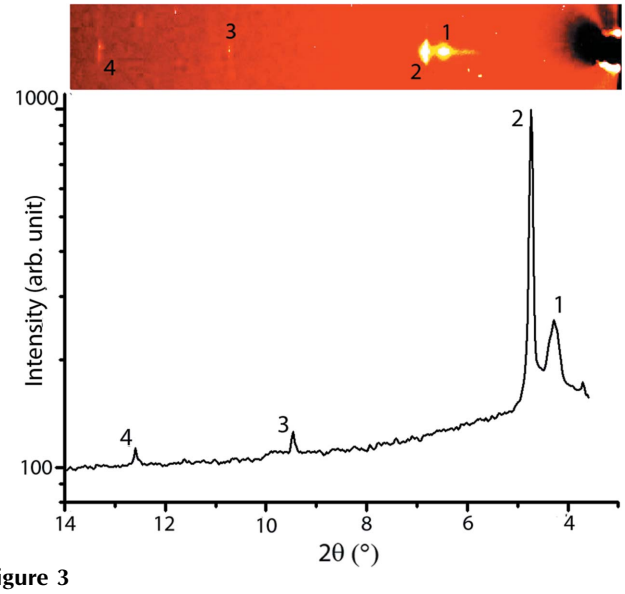

Figure 3
Top: magnification of the out-of-plane region of the GIXD diffraction pattern of a RUB thin film grown on a TEN substrate. Bottom: one-dimensional diffractogram obtained by radial integration of the two-dimensional pattern reported at the top. The numbers indicating the peaks refer to Table 1. Peak 1 originates from RUB, while the other three peaks originate from the substrate.

disposed around the main one, possibly probed by the beam during sample rotation. This is confirmed also by the fact that, collecting a series of images at different azimuthal orientations of the sample, the rings are present only in some of the images, *i.e.* when the sample is rotated such that the disordered TEN crystals enter the beam.

3.2. In-plane film orientation and epitaxial relationship with the substrate

In order to verify the existence of an in-plane order of the crystalline structure of the film, we collected a series of GIXD patterns rotating the sample by an angle of 2° around the vertical axis between two successive measurements, for a total rotation angle of 180° and a total scan time of 26205 s. If the grains constituting the film are not distributed with a random azimuthal orientation, then for each sample orientation only some of the diffraction spots should appear in the collected pattern. Plotting the intensity of a given reflection as a function of the azimuthal orientation of the sample, one can obtain a plot with one or more peaks, corresponding to the azimuthal orientations at which the reflection appears. This procedure is equivalent to collecting a pole figure for the given reflection, making it possible to gain some insight into the in-plane order of the overlayer by comparison with the simulated pole figures of the reflections under examination (Resel *et al.*, 1997, 2007; Campione *et al.*, 2006). In Fig. 4 we report the measured intensity *versus* azimuth plots for the (0 $\bar{1}$ 1) reflection of TEN and the (1 $\bar{1}$ $\bar{2}$) reflection of RUB, respectively, while in Fig. 5 we report the superposition of the simulated pole figures of those two reflections calculated for a TEN and a RUB single crystal with the (0 0 1) and the (2 0 0) planes, respectively, normal to the azimuthal rotation axis. In such diagrams the intensity of a given reflection is plotted as a function of the azimuthal angle (φ) and of the polar angle (ψ) of the reflection.

In the lower curve in Fig. 4, owing to the triclinic symmetry of the TEN unit cell, the (0 $\bar{1}$ 1) diffraction spot should appear only once for each complete revolution of the crystal around its vertical axis, as can be observed in the simulated pole figure reported in Fig. 5, showing that no reflection equivalent by symmetry to the (0 $\bar{1}$ 1) one is present. The presence of two clearly distinct peaks in the plot of Fig. 4, indicating the appearance of the (0 $\bar{1}$ 1) reflection for two different azimuthal orientations of the sample, means that the substrate is constituted of two differently oriented crystals. The angular separation between the two peaks in the plot relative to TEN (0 $\bar{1}$ 1) is 42°. This corresponds to the in-plane angle between the two orientations of the substrate. Careful observation of the substrate with a light-polarized optical microscope shows that the substrate actually consists of two differently orientated TEN single crystals that coalesced together during their growth, and that the angular difference in their orientation is equal to ∼42°.

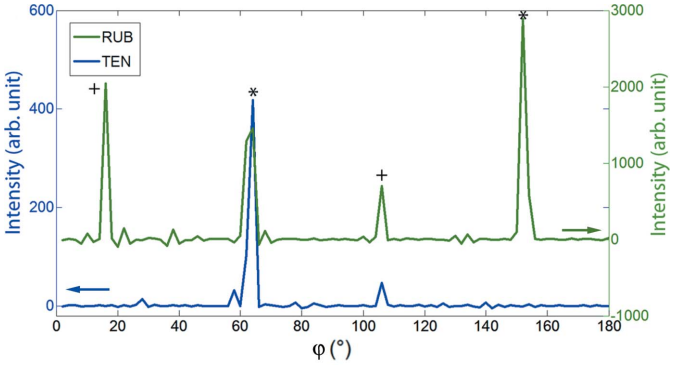

Figure 4
Measured intensity of the (1 $\bar{1}$ $\bar{2}$) reflection of the RUB thin film (upper curve) and of the (0 $\bar{1}$ 1) reflection of the TEN substrate (lower curve) as a function of the azimuthal orientation of the sample (φ). The RUB plot has been shifted to the left by 36° in order to show the correspondence between RUB and TEN reflections. The two (*) and (+) symbols indicate reflections from differently orientated crystals.

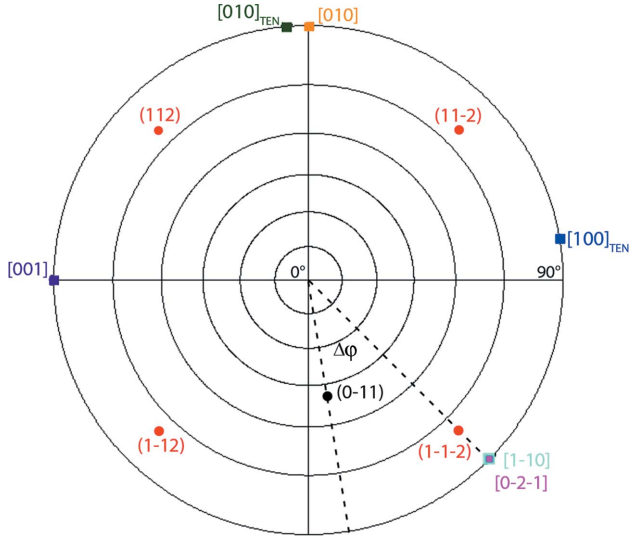

Figure 5
Superposition of the simulated pole figures of a RUB crystal with the (100) plane parallel to the image plane and of a TEN crystal with the (001) plane parallel to the image plane. The {1 1 2} and the (0 $\bar{1}$ 1) reflections are reported for RUB and TEN, respectively. The concentric circles are separated by $\Delta\psi = 15°$. The two pole figures are superimposed with an azimuth such that the azimuthal angle between the (1 $\bar{1}$ $\bar{2}$) reflection of RUB and the (0 $\bar{1}$ 1) reflection of TEN, labelled as $\Delta\varphi$, is consistent with the experimentally determined one (36°). On the outer circle (corresponding to $\psi = 90°$) the [0 1 0], [0 0 1] and [0 $\bar{2}$ $\bar{1}$] RUB direct lattice directions and the [1 0 0], [0 1 0] and [1 $\bar{1}$ 0] TEN direct lattice directions are also reported, as used in the text to determine the epitaxial relationship between the overlayer and the substrate.

In the upper curve of the graph in Fig. 4 the intensity of the (1 $\bar{1}$ $\bar{2}$) reflection of the overlayer as a function of the azimuthal orientation of the sample is plotted. In this case one can notice the presence of a few clearly defined peaks over a uniform background. This means that the RUB (1 $\bar{1}$ $\bar{2}$) reflection is present only at some specific azimuthal orientations of the sample and, thus, that the film crystalline domains are oriented along definite directions. The angular separation between two successive appearances of the (1 $\bar{1}$ $\bar{2}$) diffraction spot, or one of its symmetrically equivalent reflections, for a RUB orthorhombic single crystal is 90°, as can be observed in the simulated pole figure reported in Fig. 5. In particular the plot shows four different peaks; the separation between the

first and the third peak is 90° and equal to that between the second and the fourth peak. This means that the overlayer has two different in-plane orientations, with an angular separation between each other corresponding to that between the first and the second peak in the plot, namely 42°. The angular separation between the two different in-plane orientations of the RUB overlayer thus corresponds to the angular separation between the two different orientations of the substrate, meaning that for each orientation of the substrate there is only one possible orientation of the overlayer, *i.e.* there is a unique epitaxial relationship between the film and the substrate. The two plots reported in Fig. 4 were shifted in order to show more clearly the correspondence between the azimuthal positions of the RUB and TEN reflections. The actual angular separation between the appearance of the TEN (0 $\bar{1}$ 1) reflection and that of the successive RUB (1 $\bar{1}$ $\bar{2}$) reflection is 36 ± 2°.

Starting from the measured angular separation of 36 ± 2° between the TEN (0 $\bar{1}$ 1) and RUB (1 $\bar{1}$ $\bar{2}$) reflections, and referring to the two simulated pole figures reported in Fig. 5, on which we also plotted some relevant direct lattice directions of RUB and TEN, the exact epitaxial relationship between the two layers can now be determined. In order to do so, the two pole figures reported in Fig. 5 have been reciprocally oriented such that the angle $\Delta\varphi$ between the TEN (0 $\bar{1}$ 1) reflection and the RUB (1 $\bar{1}$ $\bar{2}$) reflection is equal to the experimentally determined one (36 ± 2°). In this way it can be clearly concluded that the experimental data are compatible with an orientation of the overlayer with respect to the substrate such that the [1 0 0] direction of the TEN lattice forms an angle of ∼80° with the [0 1 0] lattice direction of the RUB film, and the *b* axis of RUB forms an angle of ∼5° with the *b* axis of TEN. Moreover, there is a coincidence between the [0 $\bar{2}$ $\bar{1}$] and [1 $\bar{1}$ 0] lattice directions of RUB and TEN, respectively. This situation is equivalent to the epitaxial relationship RUB[0 2 1] ∥ TEN[1 $\bar{1}$ 0], previously suggested by molecular resolution atomic force microscopy results, therefore related to a local scale (Campione, 2008), and corresponds to an alignment between pronounced corrugations of the RUB (2 0 0) and TEN (0 0 1) surfaces, respectively, as shown in the structural model of Fig. 6. Such a result thus confirms the role of surface corrugation in determining the epitaxial ordering of molecular thin films (Haber *et al.*, 2008; Smilgies & Kintzel, 2009). Moreover, these measurements confirm that the RUB overlayer possesses a unique orientation on a macroscopic scale.

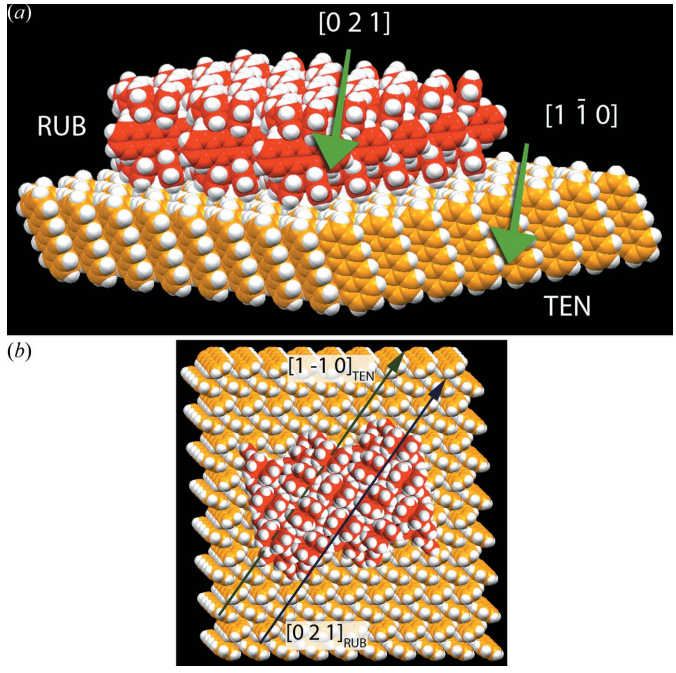

Figure 6
(*a*) Structural model of the relative arrangement of RUB film and TEN substrate molecules as deduced by the measurements described in the text. The pronounced surface molecular corrugations aligned along the [0 2 1] and [1 $\bar{1}$ 0] directions of RUB and TEN, respectively, are indicated by arrows. (*b*) Top view of the structural model reported in (*a*). The relevant directions of RUB and TEN crystals are indicated by the arrows.

4. Conclusions

The crystalline structure of RUB thin films epitaxially grown on TEN single crystals was studied with GIXD. First, it was shown that RUB grows in the thin-film form only with its orthorhombic crystalline phase and with a unique out-of-plane orientation, corresponding to RUB(2 0 0) ∥ TEN(0 0 1). Then, it was shown that the film grows with a unique in-plane orientation relative to the substrate, and finally it was possible to determine the actual epitaxial relationship between the film and the substrate, finding a perfect agreement with previously reported results for the same system (Campione, 2008). The results we reported here are also in agreement with those already reported for other all-organic epitaxial systems, confirming that highly ordered epitaxial growth of organic crystalline thin films on organic substrates can be achieved for a variety of materials, provided that the correct substrate/overlayer couple is used, and also confirming that X-ray-diffraction-based techniques are an invaluable tool for the study and characterization of such systems (Campione *et al.*, 2006; Yoshimoto *et al.*, 2008). Besides precisely determining the main structural properties of an all-organic heterostructure of great interest for the field of organic electronics, we have also shown that GIXD measurements carried out at the XRD1 beamline of the ELETTRA synchrotron facility are suitable for a fast and accurate characterization of the structural properties of organic crystalline heterostructures based on extremely thin films, with a thickness equal or inferior to 20 nm.

The authors are grateful to Fondazione Cariplo (grant no. 2009/2551) for financial support.

References

Braga, D. & Horowitz, G. (2009). *Adv. Mater.* **21**, 1473–1486.
Brütting, W. (2006). *Physics of Organic Semiconductors.* Weinheim: Wiley-VCH.
Campione, M. (2008). *J. Phys. Chem. C*, **112**, 16178–16181.
Campione, M., Moret, M., Raimondo, L. & Sassella, A. (2009). *J. Phys. Chem. C*, **113**, 20927–20933.

Campione, M., Sassella, A., Moret, M., Papagni, A., Trabattoni, S., Resel, R., Lengyel, O., Marcon, V. & Raos, G. (2006). *J. Am. Chem. Soc.* **128**, 13378–13387.
Haber, T., Resel, R., Thierry, A., Campione, M., Sassella, A. & Moret, M. (2008). *Physica E*, **41**, 133–137.
Haemori, M., Yamaguchi, J., Yaginuma, S., Itaka, K. & Koinuma, H. (2005). *Jpn. J. Appl. Phys.* **44**, 3740–3742.
Hammersley, A. P. (1997). *ESRF Internal Report* ESRF97HA02T. ESRF, Grenoble, France.
Holmes, D., Kumaraswamy, S., Matzger, A. J. & Vollhardt, K. P. C. (1999). *Chem. Eur. J.* **5**, 3399–3412.
Hu, W. S., Weng, S. Z., Tao, Y. T., Liu, H. J. & Lee, H. Y. (2008). *Org. Electron.* **9**, 385–395.
Jurchescu, O. D., Meetsma, A. & Palstra, T. T. M. (2006). *Acta Cryst.* B**62**, 330–334.
Käfer, D. & Witte, G. (2005). *Phys. Chem. Chem. Phys.* **7**, 2850–2853.
Klauk, H., Halik, M., Zschieschang, U., Schmid, G., Radlik, W. & Weber, W. (2002). *J. Appl. Phys.* **92**, 5259.
Lan, M., Xiong, Z.-H., Li, G.-Q., Shao, T.-N., Xie, J.-L., Yang, X.-F., Wang, J.-Z. & Liu, Y. (2011). *Phys. Rev. B*, **83**, 195322.
Laudise, R. A., Kloc, C., Simpkins, P. G. & Siegrist, T. (1998). *J. Cryst. Growth*, **187**, 449–454.
Podzorov, V., Menard, E., Borissov, A., Kiryukhin, V., Rogers, J. A. & Gershenson, M. E. (2004). *Phys. Rev. Lett.* **93**, 086602.
Rand, B. P., Genoe, J., Heremans, P. & Poortmans, J. (2007). *Prog. Photovolt.* **15**, 659–676.
Resel, R., Koch, N., Meghdadi, F., Leising, G., Unzog, W. & Reichmann, K. (1997). *Thin Solid Films*, **305**, 232–242.
Resel, R., Lengyel, O., Haber, T., Werzer, O., Hardeman, W., de Leeuw, D. M. & Wondergem, H. J. (2007). *J. Appl. Cryst.* **40**, 580–582.
Salzmann, I. & Resel, R. (2004). *J. Appl. Cryst.* **37**, 1029–1033.
Sassella, A., Campione, M. & Borghesi, A. (2008). *Riv Nuovo Cim.* **31**, 457–490.
Smilgies, D.-M. & Blasini, D. R. (2007). *J. Appl. Cryst.* **40**, 716–718.
Smilgies, D.-M., Blasini, D. R., Hotta, S. & Yanagi, H. (2005). *J. Synchrotron Rad.* **12**, 807–811.
Smilgies, D. & Kintzel, E. J. (2009). *Phys. Rev. B*, **79**, 235413.
Tate, M. P., Urade, V. N., Kowalski, J. D., Wei, T. C., Hamilton, B. D., Eggiman, B. W. & Hillhouse, H. W. (2006). *J. Phys. Chem. B*, **110**, 9882–9892.
Wöll, C. (2009). *Physical and Chemical Aspects of Organic Electronics.* Weinheim: Wiley-VCH.
Yamashita, Y. (2009). *Sci. Technol. Adv. Mater.* **10**, 024313.
Yoshida, H. & Sato, N. (2006). *Appl. Phys. Lett.* **89**, 101919.
Yoshimoto, N., Kakudate, T., Aosawa, K. & Saito, Y. (2008). *J. Cryst. Growth*, **310**, 1725–1728.